FINE-SCALE FILAMENTARY STRUCTURE IN CORONAL STREAMERS

Richard Woo and John W. Armstrong

Jet Propulsion Laboratory, California Institute of Technology, Pasadena, California

Michael K. Bird

Radioastronomisches Institut, Universität Bonn, Bonn, Germany

Martin Pätzold

Institut für Geophysik and Meteorologie, Universität zu Köln, Germany

ABSTRACT

Doppler scintillation measurements of a coronal streamer lasting several solar rotations have been conducted by Ulysses in 1991 over a heliocentric distance range of 14–77 $R_\odot$. By showing that the solar corona is filamentary, and that Doppler frequency is the radio counterpart of white-light eclipse pictures processed to enhance spatial gradients, it is demonstrated that Doppler scintillation measurements provide the high spatial resolution that has long eluded white-light coronagraph measurements. The region of enhanced scintillation, spanning an angular extent of 1.8° in heliographic longitude, coincides with the radially expanding streamer stalk, and represents filamentary structure with scale sizes at least as small as 340 km (0.5 arcsec) when extrapolated to the Sun. Within the stalk of the streamer, the fine-scale structure corresponding to scale sizes in the range of 20–340 km at the Sun and associated with closed magnetic fields, amounts to a few percent of the mean density, while outside the stalk, the fine-scale structure associated with open fields is an order of magnitude lower. Clustering of filamentary structure that takes place within the stalk of the streamer is suggestive of multiple current sheets. Comparison with ISEE-3 in situ plasma measurements shows that significant evolution due to dynamic interaction with increasing heliocentric distance takes place by the time streamers reach Earth orbit.

1. INTRODUCTION

Coronal streamers, the most conspicuous large-scale quasi-stationary features of the solar corona, have been extensively observed in white - light measurements as well as investigated theoretically (Koutchmy & Livshits 1992; Poletto 1994; Kopp 1994; Guhathakurta & Fisher 1995). Rising above the neutral line that separates the large-scale positive and negative polarity regions of the coronal magnetic field, streamers extend into interplanetary space, appearing as density enhancements near the heliospheric current sheet at 1 AU (Gosling et al. 1981; Huddleston et al. 1995).

Recent investigations based on Doppler scintillation measurements have shown that enhancements in electron density fluctuations near the neutral line and hence the heliospheric current sheet are the interplanetary manifestation of coronal streamers in the vicinity of the Sun (Woo et al. 1994, 1995). The purpose of this paper is to use S- and X-band (wavelengths of 13 and 3.6 cm) radio propagation measurements conducted by Ulysses during its solar conjunction in 1991 (Bird et al. 1994) to show that (1) these enhancements coincide with the stalks of coronal streamers as observed in solar eclipse pictures when processed to enhance spatial gradients (Koutchmy 1975), (2) the fluctuations represent fine-scale filamentary structure, and (3) the filamentary structure undergoes significant evolution with increasing heliocentric distance by the time it reaches Earth orbit.

2. ULYSSES RADIO PROPAGATION MEASUREMENTS

This paper is based on radio propagation measurements of ranging (time delay $\Delta\tau$) and Doppler frequency. Ranging or time delay $\Delta\tau$ observes path integrated electron density n

$$\Delta\tau \sim \int n \, ds \tag{1}$$

and Doppler frequency f_D the time derivative of path integrated density

$$f_D \sim \frac{d}{dt}\int n \, ds \tag{2}$$

wheres is distance along the ray path. Doppler scintill alien σ_D is the rms of Doppler frequency fluctuations estimated for some time scale. For a spherically symmetric solar wind, ranging essentially probes the mean density n (Bird et al. 1994), and Doppler scintillation density fluctuations An (Woo 1978) near the closest approach of the radio path.

The Ulysses conjunction is wel]-suited for investigating coronal streamers, because it took place at a time when the large-scale coronal magnetic field was stable, and the tilt of the heliospheric current sheet large enough that recurrent low-latitude coronal streamers persisted over several solar rotations, thus permitting measurements at varying heliocentric distances. Onc of these streamers located near Carrington longitude 350° was identified in the Ulysses S-band 5-hour ranging and ranging scintillation measurements (Woo et al., 1995). First detected off the cast limb on DOY 228 (16 August 1991), this streamer was seen again half a solar rotation later on DOY 240 (28 August 1991) when the Ulysses radio path had crossed over to the west limb.

Shown in Fig. 1 arc the S-band measurements of this same streamer on DOY 228 and 240, consisting of 10-rein time delay $\Delta\tau$ (Bird et al. 1994) and 3-min Doppler scintillation σ_D based on 10-see Doppler data (Woo et al. 1985), and plotted over a period of 0.6 day (14.4 hrs). Note that the time axes arc shown in reverse to coincide with solar synoptic maps, for which increasing Barrington longitude usually runs from left to right. Fractional density fluctuation An/n is estimated once every 3 mins by converting Doppler scintillation to ranging scintillation before dividing by the corresponding 10-min ranging measurement. in the conversion, it is assumed that the electron density spectrum is power-law and Kolmogorov (one-dimensional spectral index of 5/3). The results arc not sensitive to the spectrum shape as they differ by only 16% over the range of observed spectral indices — 5/3 to 1 (Woo and Armstrong 1979).

As found previously with 5-hr averages of ranging and ranging scintillation based on 10-min ranging measurements (Woo et al. 1995), enhancements in density n ($\Delta\tau$), density fluctuation An (σ_D) and An/n arc the manifestation of the streamer crossing, but those of

An and An/n are strikingly higher than that of the mean or large-scale density. For instance, in the case of DOY 240, n rises by a factor of two, while An and An/n rise by a factor of about 50. in the enhanced region, An/n is as high as a few percent. The boundaries of the enhanced regions of An and An/n are also more abrupt than those of the mean or large-scaic density, suggesting the separation of small-scale plasma of different nature and origin.

At first glance, the abruptness of the path-integrated scintillation measurements suggests temporal rather than spatial variation, but spat ial variation is confirmed by the similarity in the scintillation time series during successive solar rotations, as shown in Figs. 2b and 2c. These results show that the region of enhanced density fluctuations corresponds to a flow t ube (or sheet since path-integrat ed measurements cannot distinguish between flow tube and sheet) of angular extent 1.8° in heliographic longitude. Furthermore, clustering of filamentary structure within this flow tube is evident, as there appears to be as many as three smaller flow tubes that are not only long-lived but extend from 14 to 77 R_o. The 3-min sampling rate of' the Doppler scintilla ion data indicates that the filamentary structure extends to sizes as small as 340 km at the Sun (0.5 arcsec). The flow tube's angular size as measured by the duration of the enhance.(i scintillation changes little over this heliocentric distance range, indicating approximate radial expansion. When extrapolated back to the Sun, the size of the largest flow tube is 2 x 10^4 km (30 arcsec) and that of the smaller ones is 7300 km (10 arcsec). The three inner t ubes suggest three current sheets that arc associated with twin- or three-wch helmet streamers (Crooker et al. 1993). in situ plasma measurements near 0.3 AU by Helios, showing pressure.-balanceci structures in the slow solar wind (Thieme et al. 1990), is also consistent with the filamentary structure found near the Sun.

3. RELATIONSHIP OF RAD1O TO WHITE-LIGHT MEASUREMENTS

White-]ight pictures of streamers in the outer corona, like the ranging results in Fig. 1, show density profiles that are relatively smooth, and exhibit relatively low contrasts between tbc interior and exterior of the streamer. This is of course expected, as both white-light and ranging observe path-integrated electron density. When the same white-light pictures are processed to remove the radial dependence and enhance spatial gradients of the corona, they reveal a variety of striking ray-like structures (Koutchmy et al. 1975; Guhathakurta and Fisher 1995). Parallels between Doppler scintillation and white-light measurements arc clear as soon as it is realized that the density fluctuations observed by Doppler scintilla ion represent filamentary structure. Variations in the Doppler scintillation indeed become more evident once the dominant radial dependence is removed (Woo and Gazis 1993; Woo et al. 1994). However, they arc more abrupt and dramatic than the ringing variations because, like the ray-like structure in the enhanced white-light pictures, they arc the manifestation of the gradient in path-integrated density. Since Doppler frequency measures the time derivative of path-integrated density given by equation (2), for filamentary structure, it is also measuring the spatial gradient related to the time derivative through the Sun's rotation rate.

Examination of the Ulysses 1-sec dual-frequency Doppler time series (Woo et al. 1976) shows density gradients of signs that arc alternating approximately continuously, suggesting that filamentary structure extends down to the smallest corresponding size of 3×10^{-3} arcsec (2 km) at the Sun. Recent interpretation of angular broadening measurements that image the electron density irregularities in the plane of the sky confirms filamentary structure at least as small as 1 km (Woo 1995b). Thus, the ?-rein Doppler scintillation measurements that arc based on 10-see Doppler samples correspond to the rms of spatial gradients computed over a distance of 340 km at the Sun (0.5 arcsec) based on measurements of the gradient every 20 km (3 x 10-2 arcsec).

The regions of enhanced Doppler scintillation, of roughly the same size (1–20), obviously coincide with the stalks of the coronal streamers in eclipse pictures processed to similarly reveal spatial gradients, These enhanced eclipse pictures show that the gradient of onc boundary of the stalk is often greater than that of the other. A similar situation is also evident in Fig. 1 showing steeper gradients on the eastern and western boundaries of the stalk on DOY 228 and DOY 240, respectively. Of course, it is their high time resolution that translates Doppler scintillation into high spatial resolution measurements, thereby revealing fine-scale filamentary structurc in the stalks not observed in white-light measurements. Recent results on velocity structure in the inner corona deduced from multiple-station intensity scintillation measurements over the streamer belt suggest that these streamer stalks are most likely the sources of the slow solar wind (Woo 1995a).

Finally, while long-lived filamentary structure is observed in Fig. 2, the results in Fig. 1 show that considerable variation in both large- and small-scale structure of the streamer can take place over a period of half a solar rotation. Amongst others, there is a shift of the steeper density gradient from the eastern to western flank. Such temporal changes arc also consistent with those of large-scale coronal streamer structure seen in white-light measurements (Poland 1978).

4. EVOLUTION WITH HELIOCENTRIC DISTANCE

For heliocentric distances beyond 77 R_o, only X-band measurements of the coronal streamer at Barrington longitude 350° were available, and these are shown in Figs. 2a and 2c. Multiplication of the X-band measurements σ_D by the factor (3/11)x $\sqrt{2}$ converts them to an approximate correspondence with the S-band measurements of Figs. 2b-2d. Although the time series in Figs. 2a and 2c do not cover the full duration of streamer passage, they nevertheless hint at erosion and expansion of the enhanced region of density fluctuations with increasing heliocentric distance. A more complete. and representative X-band profile near Earth orbit is that of another streamer near Carring ton longitude 190°

displayed in Fig. 2f, showing that the region of enhanced density fluctuations has grown to an angular width of about 8° near 1 AU. Insight into the evolution of the Doppler scintillation streamer signature is provided by results from a superposed epoch analysis of heliospheric current sheet (HCS) crossings at 1 AU bawd on 1 -hr averages of S-rein field and particle measurements by ISEE-3 (Huddleston et al. 1995). The density fluctuation results from this ISEE-3 study have been superimposed on the scintillation results in Fig. 2f, showing a remarkable consistency between the two measurements. This shows that, as the fast wind runs into the slow wind, dynamic leading-e.dgc compression causes broadening of the region of density fluctuations, particularly to the east of the HCS. Thus, densit y fluctuation enhancements associated with corot sting interaction regions formed farther from the Sun are often difficult to distinguish from coronal streamers (Ananthakrishnan et al. 1980; Houminer and Furguson 1993).

5. DISCUSSION AND CONCLUSIONS

The electron density irregularities investigated by Doppler (or phase) scintillation measurements near the Sun over the past two decades have been generally thought of as turbulent in nature. That they represent filamentary structure instead is somewhat surprising. This new perspective, however, elucidates the parallels between Doppler scintillation measurements and eclipse pictures that have been processed to enhance spatial gradients, reinforces the observations of ray-like structures in the enhanced eclipse pictures, explains the abrupt variations in Doppler scintillation that coincide with the stalks of coronal streamers, and improves our understanding, of in situ plasma measurements of the heliospheric current sheet at 1 AU. More important, Doppler scintillation measurements offer the higher spatial resolution that has so far eluded coronal imaging (Koutchmy et al. 1994). This improved resolution has revealed that the stalks of coronal streamers, which are most likely the sources of the slow solar wind, are permeated by fine-scale filamentary structure. Although high spatial resolution is a consequence of the high time resolution, it is the high sensitivity and wide dynamic range. of the Doppler measurements that have made it possible to observe the fine-scale structure in and out of the streamer stalk. These are the same features that have enabled Doppler scintillation measurements to observe the solar wind and its variations over a heliocentric distance range that spans from the vicinity of the Sun to near Earth orbit (Woo 1978).

Small-scale coronal structure has received much attention lately (see e.g., Habbal 1992), The Ulysses Doppler scintillation measurements show that small-scale structure for scale sizes in the range of 20–340 km amounts to only a few percent of the large-scale density, even within the stalk of the streamer, where it is largest. Still, the importance and need for high spatial resolution measurements is poignantly demonstrated by the fact that the range of variation of small-scale structure is far greater than that of the large-scale density. Thus, within the stalk of the streamer, the structure associated with closed magnetic fields is an order of magnitude larger than that outside the stalk associated with open fields. Clustering of the filamentary structure within the streamer stalk is probably a manifestation of multiple current sheets. With Yohkoh already providing X-my images (Ogawara cl al. 1992; Strong et al. 1992) and SOHO soon to provide enhanced spectroscopic and white-light imaging capabilities (sec e.g., Brueckner ct al. 1992), probing small-scale coronal structure with complementary Doppler scintillation measurements by e.g., Galileo and ICE (Woo 1994), opens up new and exciting opportunities for improving our understanding of small-scale structure and its relationship to solar and coronal features.

It is a pleasure to acknowledge the outstanding support received from the Ulysses Project and the NASA DSN. Wc arc especially grateful to C. Chang for programming and data processing, and to S. Asmar, A. Devereaux, P. Eshe, R. Herrera, R. Horton and D. Morabito for support. This paper presents results of a research project partially funded by the Deutsche Agentur für Raumfahrtangelegenheiten (DARA) GmbH under the contracts

50 ON 9104 and 50 ON 9401, and describes research carried out at the Jet Propulsion Laboratory, California Institute of Technology, under a contract with NASA. The responsibility for the contents of this publication is assumed by the authors,

REFERENCES

Ananthakrishnan, S., Colts, W.A. & Kaufman 1980, J. Geophys. Res. 85, 6025

Bird, M. K., Volland, H., Pätzold, M., Edenhofer, P., Asmar, S. W., & Brenkle, J.P. 1994, Ap. J., 426, 373

Brueckner, G., & et al. 1992, ESA SP-348, 27

Crooker, N. U., Siscoe, G.L., Shodhan, S., Webb, D.F., Gosling, J.T., & Smith, E.J. 1993, J. Geophys. Res., 98, 9371

Gosling, J.'I'., Borrini, G., Asbridge, J. R., Bame, S, J., Feldman, W. C., & Hansen, R.T. 1981, J. Geophys. Res., 86, 5438

Guhathakurta, M., & Fisher, R. 1995, Geophys. Res. Letters, submitted

Habbal, S.R. 1994, Space Sci. Rev., 70, 37

Houminer, Z., & Gallagher, F. 1993, Solar Phys., 145, 359

Huddleston, D. E., Woo, R., & Neugebauer, M. 1995, J. Geophys. Res., in press

Kopp, R.A. 1994, Space Sci. Rev. 70, 309

Koutchmy, S. 1975, Solar Phys., 51, 399

Koutchmy, S., & Livshits, M. 1992, Space Sci. Rev., 61, 393

Koutchmy, S. & et al. 1994, Astron. Astrophys., 281,249

Ogawara, Y., et al. 1992, Publ. Astron. Sot. Japan, 44, L41

Poland, A,]. 1978, Solar Phys., 57, 141

Poletto, G. 1994, Space Sci. Rev. 70,241

Strong, K. T., & et al. 1992, Publ. Astron. Soc. Japan, 44, 1.16]

Thieme, K. M., Marsch, E., & Schwenn, R. 1990, Ann. Geophys., 8, 713

Woo, R. 1978, Ap. J., 219, 727

Woo, R. 1994, ESA SP-373, 239

Woo, R. 1995a, Geophys. Rcs. Lett., in press

Woo, R. 1995b, Nature, submitted

Woo, R., & Gazis, P.R. 1993, Nature, 366, 543

Woo, R., & Armstrong, J.W. 1979, J. Geophys. Rcs. 84, 7288

Woo, R., Armstrong, J. W., & Gazis, P.R. 1994, Space Sci. Rev., 72, 223

Woo, R., Yang, F.-C., Yip, K, W., & Kendall, W.B. 1976, Ap. J. 210, 568

Woo, R., Armstrong, J. W., Bird, M. K., & Pätzold, M. 1995, Geophys. Rcs. Lett., 22, 329

Woo, R., Armstrong, J. W., Sheeley, Jr., N. R., Howard, R. A., Koomen, M. J., Michels, D. J., & Schwenn, R. 1985, J. Geophys. Res., 90, 154

FIGURE CAPTIONS

Figure 1. Profiles of $\Delta\tau$ (-n) and σ_D (-An) of coronal streamer near Carrington longitude 350°. For the sake of comparison, all plots cover 0.6 day. Figs. 1a and 1b took place on the east limb, while Figs. 1c and 1d on the west limb half a solar rotation later. Note that the streamer shows considerable variation in structure over half a solar rotation,

Figure 2. Figs. 2a-2e are profiles of σ_D (-An) of coronal streamer near Carrington longitude 350° during successive solar rotations. Fig. 2f is of corona] streamer at Barrington longitude 190°, For the sake of comparison, all plots cover 0.6 day. Except for Figs. 2b and 2c, no effort has been made to align the streamer enhancements. Figs. 2a-2c arc cast limb, and Figs. 2d-2e are west limb observations. Day of year (DOY) in Figs. 2a-2e is in 1991 while DOY in Fig. 2f is in 1992. Two regions of Fig. 2b and 2c are shaded to indicate filamentary structure lasting one solar rotation, Superimposed curve in Fig. 2f represents density fluctuation results from superposed epoch analysis of heliospheric current sheet crossing by Huddleston et al. (1 995). These results are displayed relative to the current sheet crossing as indicated at the top of the plot.

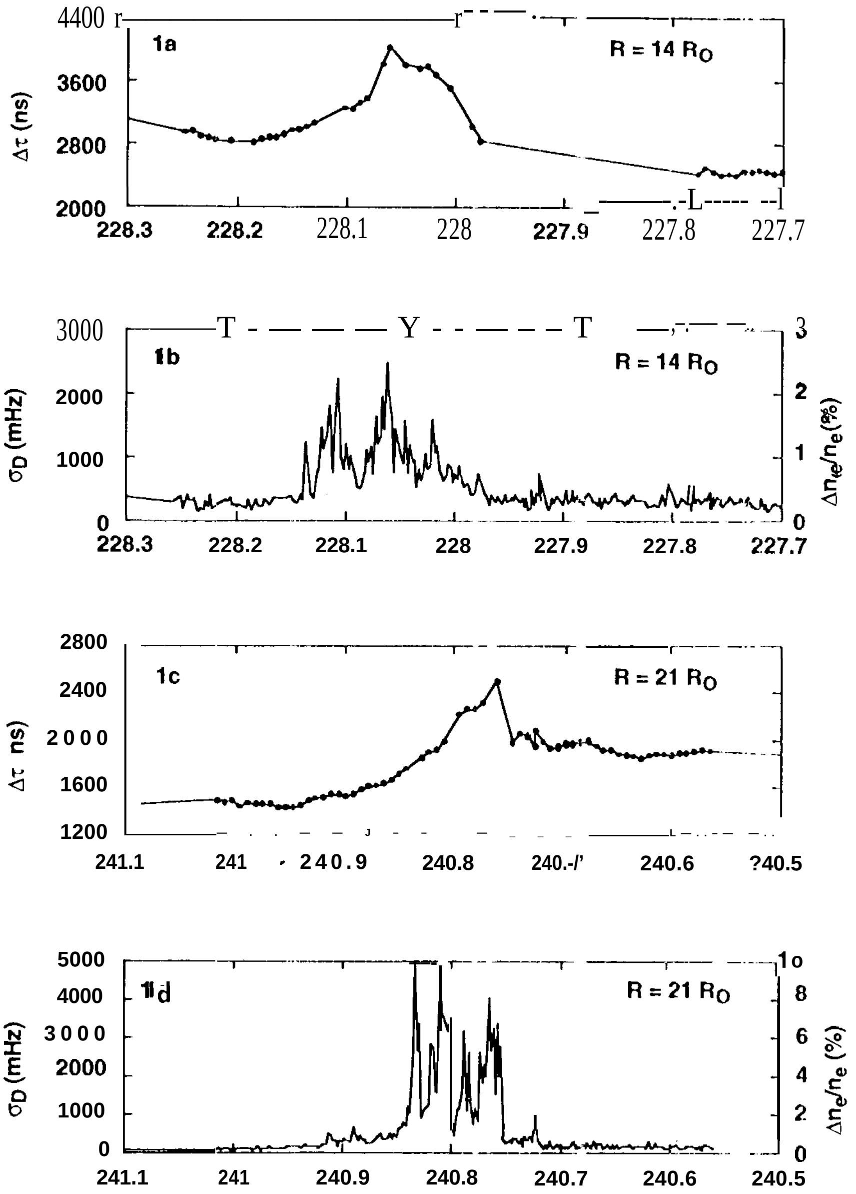
1a
R = 14 R_O
$\Delta\tau$ (ns)
4400
3600
2800
2000
228.3
228.2
228.1
228
227.9
227.8
227.7
1b
R = 14 R_O
σ_D (mHz)
$\Delta n_{le}/n_e$(%)
3000
2000
1000
0
3
2
1
0
228.3
228.2
228.1
228
227.9
227.8
227.7
1c
R = 21 R_O
$\Delta\tau$ ns)
2800
2400
2000
1600
1200
241.1
241
240.9
240.8
240.-/'
240.6
?40.5
1d
R = 21 R_O
σ_D (mHz)
$\Delta n_e/n_e$ (%)
5000
4000
3000
2000
1000
0
1o
8
6
4
2
0
241.1
241
240.9
240.8
240.7
240.6
240.5

Fig 1

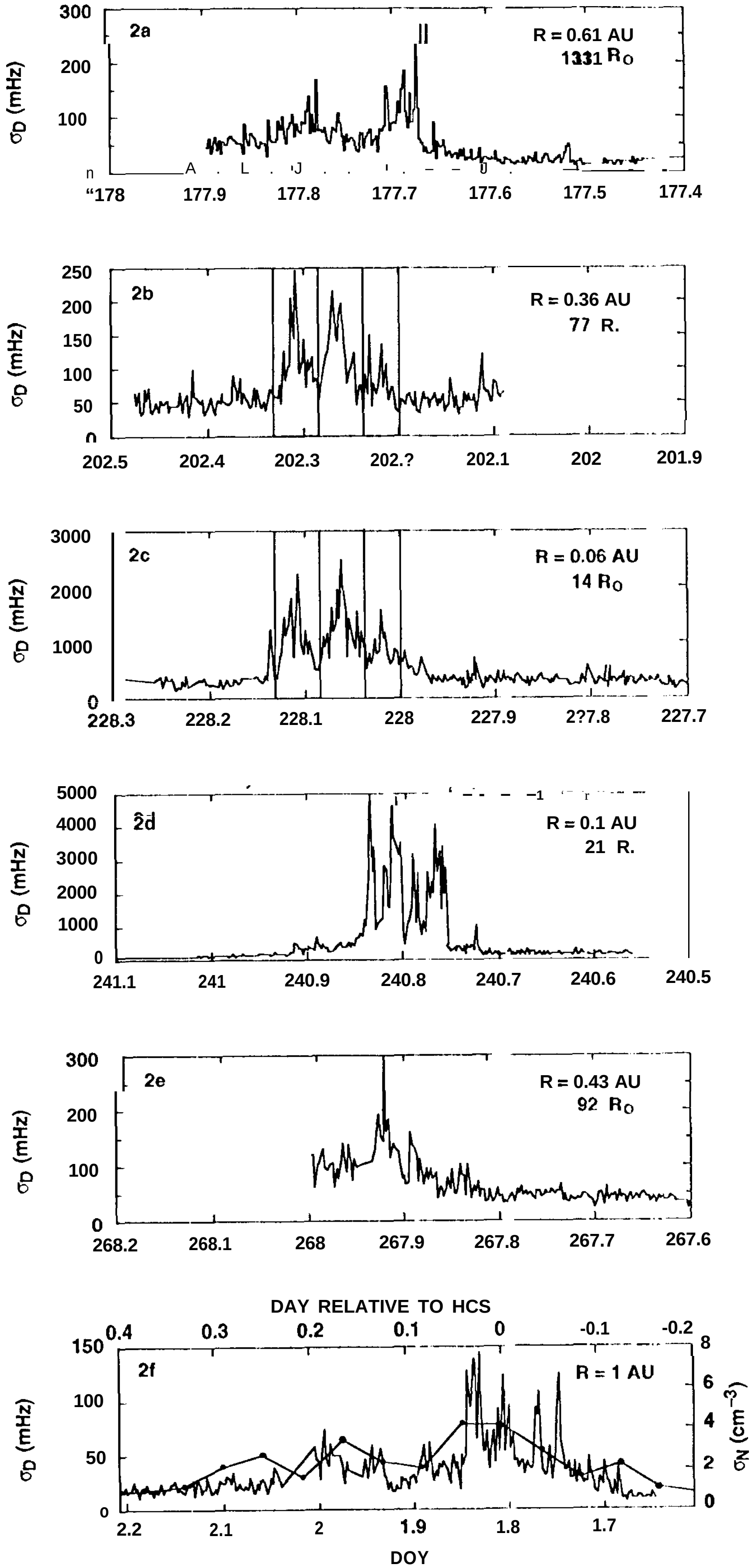
2a
R = 0.61 AU
131 R_O
2b
R = 0.36 AU
77 R.
2c
R = 0.06 AU
14 R_O
2d
R = 0.1 AU
21 R.
2e
R = 0.43 AU
92 R_O
2f
R = 1 AU
DAY RELATIVE TO HCS
DOY
σ_D (mHz)
σ_N (cm^{-3})
0.4
0.3
0.2
0.1
0
-0.1
-0.2
178
177.9
177.8
177.7
177.6
177.5
177.4
202.5
202.4
202.3
202.?
202.1
202
201.9
228.3
228.2
228.1
228
227.9
2?7.8
227.7
241.1
241
240.9
240.8
240.7
240.6
240.5
268.2
268.1
268
267.9
267.8
267.7
267.6
2.2
2.1
2
1.9
1.8
1.7

Fig. 2